Scientific Research Publishing

Open Journal of Applied Sciences, 2024, 14, 1691-1714
https://www.scirp.org/journal/ojapps
ISSN Online: 2165-3925
ISSN Print: 2165-3917

Predictive Study of Trace Metal Pollution of Gold Panning Sites in Birimian Formations: Case of the Yaouré Furrow (Côte d'Ivoire)

Tonga Paul Tiemoko[1*], Gbele Ouattara[1], Kouassi Ernest Ahoussi[2]

[1]Laboratoire des Sciences Géographiques, du Génie Civil et des Géosciences, Institut National Polytechnique Félix Houphouët-Boigny (INP-HB), Yamoussoukro, Côte d'Ivoire
[2]Laboratoiredes Sciences du Sol, del'Eauetdes Géomatériaux, Université Félix Houphouët-Boigny (UFHB), Abidjan-Cocody, Côte d'Ivoire
Email: tonga.tiemoko@inphb.ci

How to cite this paper: Tiemoko, T.P., Ouattara, G. and Ahoussi, K.E. (2024). Predictive Study of Trace Metal Pollution of Gold Panning Sites in Birimian Formations: Case of the Yaouré Furrow (Côte d'Ivoire). *Open Journal of Applied Sciences, 12,* 1691-1714.
https://doi.org/10.4236/ojapps.2024.147110

Received: May 30, 2024
Accepted: July 16, 2024
Published: July 19, 2024

Abstract

The present study was carried out on small-scale gold mining sites in the Yaouré region of Côte d'Ivoire. This region is geologically representative of the Birimian formations (2.1 Ga) of West Africa. The aim is to determine the potentially toxic trace metals (TMEs) generated by these sites, with a view to preventing possible contamination and/or metal pollution of the waters that provide fish products for local populations. To this end, a sampling campaign was carried out, resulting in the collection of 20 mining waste samples analyzed by X-ray fluorescence spectrometry (XRF) and 10 by X-ray diffractometer (XRD). The XRF analysis detected 06 predominant TMEs: arsenic, chromium, copper, nickel, zinc and vanadium. Statistical analysis was carried out to determine the distributions and correlations between these ETMs. To assess contamination and/or pollution levels, the following indices were calculated on the basis of reference concentrations of upper continental crust MTEs: Enrichment Factor, Geo-accumulation Index, Concentration Factor, Degree of contamination and those related to ecological risks. The results of statistical analyses and indices have shown that arsenic and chromium are the most predominant and can be, depending on the chemical form, potentially more toxic. The results of the DRX analysis show the occurrence of several minerals carrying these two MTEs, especially that of a rare mineral, Stenhuggarite, an arsenic oxide linked to hydrothermal veins. The majority of gold mining operations in West Africa are located in the birimian zone, hence the need for environmental monitoring by the relevant authorities, to prevent potential ecological risks to water and possibly health risks via the food chain.

Keywords

Small-Scale Mining, Metallic Trace Elements, Mining Discharges, Contamination, Pollution, Contamination, Pollution, Index

1. Introduction

The resurgence of gold mining in Côte d'Ivoire and its sometimes rudimentary practices have contributed in recent decades to degrading the natural environment and reducing, in the areas concerned, the amount of arable land in a country where agriculture remains the mainstay of the national economy. Despite the adoption in 2014 of a mining code that advocates, among other good governance activities, environmental protection, its application in the field still remains difficult, especially with small mines.

A statistical study by the Ivorian government in 2014 showed that twenty-four (24) of the country's thirty-one (31) regions are affected by gold panning, including the one to which the Yaouré gold province in the Bouaflé department (Central Côte d'Ivoire) belongs. In this area, the extraction and processing of ores contribute to the exposure of rocky materials, which are often sulphide-bearing, and therefore potentially vectors of acidification reactions under certain conditions.

The scale of this activity in the area can lead to environmental problems, notably the solubilization of metals in soil and water, and their indirect impact on the human environment. A number of studies have looked at environmental pollution by trace metals (MTEs) from mining sites [1]-[4]. These studies have shown that MTE pollution can irreversibly affect the ecosystem if adequate protective measures are not taken quickly [5].

Geologically, the Bouaflé region is located in the Lower Proterozoic (Birimian) with sulfide gold mineralization [6] [7] with abundant rainfall. For this reason, the present study focuses on possible contamination and/or pollution by MTEs. To this end, it aims to:

- identify the predominant MTEs at the region's mining sites, based on their complete detection at all sites by X-ray fluorescence spectrometer (XRF);
- identify the minerals carrying the aforementioned MTEs by analyzing samples with an X-ray diffractometer (XRD);
- determine the levels of contamination and/or pollution of these MTEs by calculating the following indices: Enrichment factor, Geoaccumulation index, Contamination factor, Polymetallic contamination degree, Ecological Risk Index (ERI) and Potential Ecological Risk Index (RI).

The results of the study will make it possible to predict the potential ecological and health risks associated with MTEs, making it a textbook case for all mining sites in the West African birimian.

2. Geological Overview of the Study Area

Côte d'Ivoire belongs to the West African Craton, and more precisely to the Man Ridge. It is underlain by a basement of Precambrian age, covering 97.5% of its surface area. This basement comprises an Archean (Kenema-Man) domain to the west (3600-2500 Ma) and a Paleoproterozoic (Birimian) domain, also known as the Baoulé-Mossi domain, to the east (2500-1800 Ma), separated by the Sassandra fault [8].

The Bouaflé region belongs to the Baoulé-Mossi domain, whose formations were emplaced during the Eburnian tectono-metamorphic event, a major episode of crustal accretion between 2.25 Ga and 2.05 Ga [9]-[12].

The Yaouré gold zone lies in the eastern half of the Bouaflé greenstone belt. This belt is an assemblage of volcanic, sedimentary and intrusive rocks. The rock types in the Yaouré district are, for the most part, mafic volcanic rocks, turbiditic metasedimentary rocks and fluvio-deltaic formations [13] [14]. The turbiditic flysch metasediments consist of sandstones with argillites and graphitic and conglomeratic horizons. Fluviodeltaic formations are made up of sandstones, conglomerates and argillites. The volcano-sedimentary rocks have been intruded by granodiorite-type plutonic rocks and granites. Mafic to ultramafic complexes are also present in the Yaouré trench. All these Birimian rocks have been metamorphosed into lower green schist facies (**Figure 1**).

The region is home to major gold panning sites and an industrial gold mine. The main gold-mineralized structure consists of volcanic and plutonic rocks containing disseminated sulfides (pyrite, chalcopyrite, pyrrhotite, etc.), associated with hydrothermal alteration that develops mainly along contact zones, across or along contacts between acid dyke stocks and intrusions of similar composition [6].

3. Materials and Methods

3.1. Equipment

The materials used were essentially sampling and laboratory equipment. For the sampling campaign, the equipment consisted of a 1/200,000 topographic map of the Gagnoa sheet [15], a Garmin Etrex 10 GPS, a hand shovel and plastic bags for packaging the samples taken. In the laboratory, sample preparation equipment included a Memmert-Saftel oven and a ball mill. Sample analysis equipment consisted of a Niton XL3t X-ray fluorescence spectrometer (XRF) and a GBC-EMMA diffractometer (XRD). According to Thermo Fisher Scientific Inc [16], manufacturer of XRF spectrometers, limits of detection (LOD) depend on test duration, interference/matrices and statistical confidence level. Research on Niton XL3t, XLi, XLp and XLt analyzers, with measurement times ranging from 30 seconds to 2 minutes, depending on the type of analyzer, yielded the following limit values: As (2 - 10 ppm), Cr (2 - 50 ppm), Cu (20 - 60 ppm), Ni (40 - 90 ppm), Zn (9 - 80 ppm) and V (20 - 60 ppm).

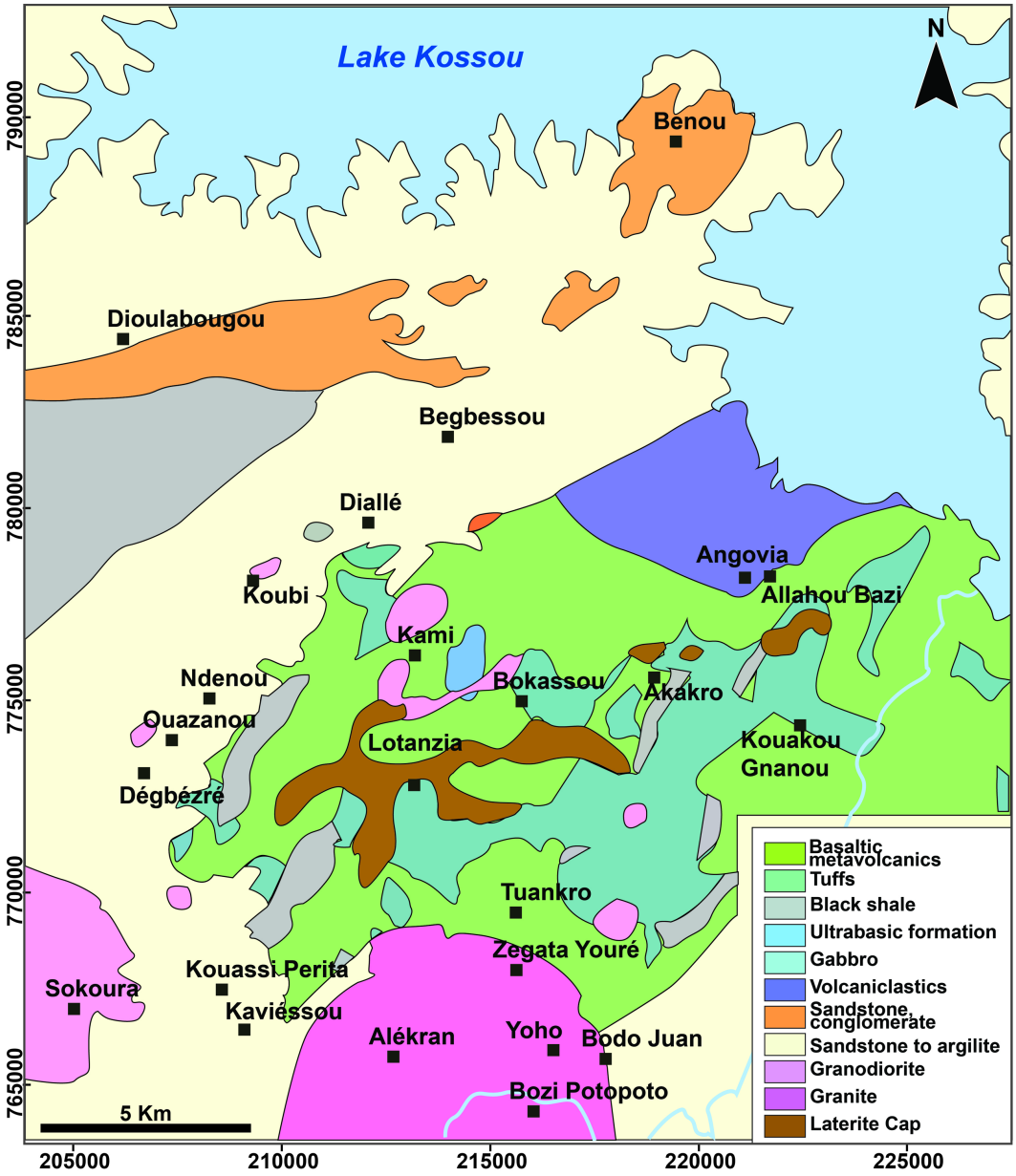

Figure 1. Geological map of Yaouré district [17].

3.2. Methods

The work methodology can be subdivided into four parts, namely sampling, preparation and XRF and XRD analysis of samples in the laboratory, statistical analysis of content data and determination, on the basis of indices, of levels and possible sources of contaminants and/or metal pollutants.

3.2.1. Sampling

The study area abounds in a multitude of sites, but not all of them are active. In fact, the activity is subject to the phenomenon of a rush to the richest areas. During the sampling period, twenty (20) localities (**Figure 2**) accounted for most of the mining activity in the Bouaflé region. They are: Alekran, Aley, Allaiyaokro,

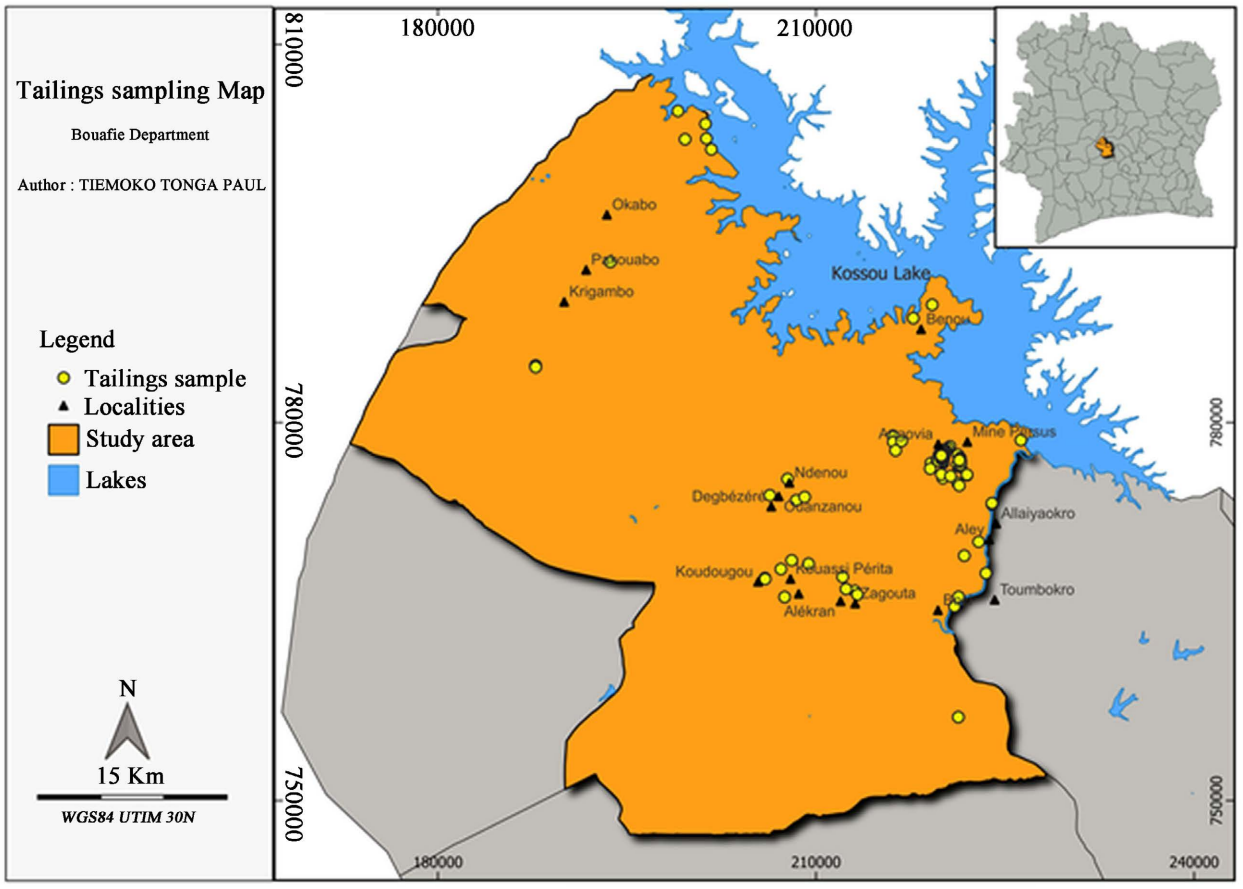

Figure 2. Sampling and study area map.

Angovia, Benou, Bozi, Degbezre, Kaviessou, Kouassi Périta, Koudougou, Ndenou, Toumbokro, Zagouta, Ouanzanou, Krigambo, Okabo Kouakougnanou and Pakouabo with its major gold mining camps of Bel chantier and Lakrikro. Each of these localities has several active sites which were sampled. For a given locality, samples from several relatively close sites were blended to form a composite sample representative of the locality.

The sampling campaign took place from February 05 to 18, 2023, during the dry season. For the XRF spectrometer analyses, samples of mine tailings were taken from the sites using a plastic hand shovel. They consisted of solid rejects (rocks, spoil heaps) and sluice slurry, and came from a variety of deposits (alluvium, eluvium, quartz veins, etc.). For XRD analysis, the samples are made up of more or less altered rocks (basalts, gabbros) (saprolite and bedrock), clays and ore processing sludges as shown in **Figure 3**. All samples collected were packaged in plastic bags and coded according to their nature and origin.

3.2.2. Sample Processing and Analysis at the Laboratory

- **Mechanical preparation for XRF analysis**

Samples were dried at 60˚C for three days in a Memmert-Saftel oven, then ground to 80% passing 75 µm. As mentioned above, an XRF spectrometer was

Figure 3. Types of samples taken at small mines: (a) Ore processing slurry; (b) Discharges from alluvial ore processing; (c) Bed-rock; (d) Saprolite-bedrock mixture.

used for concentration determination, coupled with a stand to avoid the risk of X-ray irradiation. Cups covered at their bases with 06 µm-thick Mylar sheets are filled with sample powders and placed in the stand's housing. The instrument offers the possibility of adapting measurement modes to suit the nature of the sample and the type of elements sought (major or trace elements).

In the case of our analysis, we chose the "Soil" mode, better suited to the detection of MTEs. This mode features 03 filters spaced 30 seconds apart, giving a measurement time of 90 seconds per sample. After analysis, the content data are collected on the computer using the Niton Data Transfer (NDT) software associated with the spectrometer.

- **Mechanical preparation for XRD analysis**

The samples collected undergo the same mechanical treatment as those used for XRF analysis. They are then mounted, which consists of placing the powder in a glass sample holder and aligning it precisely in the XRD measuring device. Calibration is then carried out using a reference sample, crystalline silica. Finally, the DRX device is switched on to collect diffraction data. Ten (10) samples selected on the basis of their heterogeneity were subjected to XRD analysis.

3.2.3. XRF Analysis Data Interpretation Methods

Raw assay data were sorted by eliminating major elements (except titanium, which will be used as a normalizing element in index calculations) and trace elements that were not or only partially detected, to retain only those elements with assays above the instrument's detection limits at all sites. It should be noted that several measurements were carried out on the same sample to retain the average content.

Next, monovarietal statistics were performed using XL-STAT software to determine the basic descriptive parameters of the population studied (central tendencies and dispersions). Multivariate descriptive statistics were used to determine correlations between chemical elements and to perform a principal component analysis (PCA). PCA is used to summarize the information provided by the study's MTEs (quantitative variables) and localities (individuals). To do this, the eigenvalues of the variables were determined in order to identify the main components, using Kaizer's criterion (positive values). Next, a cone diagram was designed to better visualize the eigenvalues. The analysis continued with the correlations between the variables. All these parameters led to the representation of correlation circles and visualization of the importance of each explanatory variable for each axis of representation, in particular, the relationships between mining sites and ETMs.

3.2.4. Methods for Interpreting XRD Analysis Data

When X-rays interact with matter, they cause a displacement of the electron cloud relative to the nucleus in atoms. These oscillations induce the re-emission of electromagnetic waves of the same frequency, a phenomenon known as Rayleigh scattering. The analysis parameters are as follows: Current: 28 mA; Voltage: 20 kV; Power: 1 kW and filament amperage: 4.5 mA. The interference of the scattered rays is alternately constructive or destructive, forming diffraction peaks. The relationship between the position of the peaks and the crystal lattice is described by Bragg's law, according to the following formula:

$$n\lambda = 2d\sin(\theta) \tag{1}$$

In this formula,

- n is the order of reflection,
- λ is the X-ray wavelength,
- d is the inter-reticular distance (between two crystallographic planes), and is the half-angle of deviation.

Crystalline phases are identified by analyzing the diffraction signature specific to each crystalline phase, each forming a characteristic diffraction pattern.

3.2.5. Index Calculations

Four (04) indices were calculated on the basis of reference concentrations in the Upper Continental Crust (UCC) of the ETMs selected for the study [18]. These are the Geoaccumulation index (Igeo), the Enrichment Factor (EF), the Contamination Factor (CF) and the Polymetallic contamination degree (CD). According to [19], the notion of "background noise" or "back ground", which refers to the concentration of a chemical element without human input, poses a number of problems in more or less anthropized environments. Citing [20], he recommends that the use of the term "geochemical background", which is too complex, should therefore be abandoned in favor of the concentration of trace metal elements in the upper continental crust as the geochemical reference background as shown in **Table 1**.

Table 1. Heavy metal concentrations in the upper continental crust (UCC) [18].

Chemicalelement	As	Zn	Cu	Ni	Cr	V	Ti
UCC content (ppm)	2	52	14.3	18.6	35	53	3117

- **Geoaccumulation Index (Igeo)**

The Igeo is a criterion for assessing pollution intensity [21] [22]. This empirical index compares a given concentration with the geochemical background. Igeo is calculated according to the following formula:

$$\text{Igeo} = \log_2\left[(\text{Cn})/1.5(\text{Bn})\right] \tag{2}$$

With:

- Cn: measured element concentration,
- Bn: reference concentration of the element.

The coefficient 1.5 is a correction factor to account for heterogeneity in background levels caused by lithological effects.

For the interpretation of Igeo values, Müller proposed 07 classes defined in **Table 2**.

Table 2. Interpretation of Igeo values.

Class	Value	Interpretation
7	Igeo ≥ 5	Extremely polluted
6	4 ≤ Igeo < 5	From heavily polluted to extremely polluted
5	3 ≤ Igeo < 4	Heavily polluted
4	2 ≤ Igeo < 3	From Moderately to heavily polluted
3	1 ≤ Igeo < 2	Moderately polluted
2	0 ≤ Igeo < 1	From unpolluted to moderately polluted
1	Igeo < 0	Unpolluted

- **Enrichment factor (EF)**

The enrichment factor highlights the origin of an element in sediments [23], and has been proposed to discriminate between anthropogenic and natural terrigenous inputs. In this work, the normalizing element is titanium due to its low mobility [24] and abundance in the samples. The enrichment factor is expressed by the following formula:

$$\text{EF} = \left[(\text{CMs}/\text{CNs})/(\text{CMr}/\text{CNr})\right] \tag{3}$$

With:

- CMs = concentration of metal M in the sample;
- CNs = concentration of the normalizing element in the sample;
- CMr = concentration of metal M in reference material;
- CNr = concentration of normalizing element in reference material.

For the interpretation of EF values, [23] proposed 05 classes defined in **Table 3**.

Table 3. Interpretation of EF values.

Class	Value	Interpretation
5	EF ≥ 40	Extreme enrichment
4	20 ≤ EF < 40	Moderately severe enrichment
3	5 ≤ EF < 20	Moderate enrichment
2	2 ≤ EF < 5	Minor enrichment
1	EF < 2	No enrichment

- **Contamination Factor (CF)**

CF is an excellent tool for monitoring the contamination of an environment by trace metals. It is an index that highlights the presence or absence of contamination, but also provides information on the level of contamination [25]. It is calculated using the following formula:

$$CF = (Cn/Bn) \quad (4)$$

With:

- Cn: concentration of the element in the sample;
- Bn: reference concentration of the element.

For the interpretation of CF values, Hänkanson proposed 04 classes defined in Table 4.

Table 4. Interpretation of CF values.

Class	Value	Interpretation
4	CF ≥ 6	Very high contamination
3	3 ≤ CF < 6	High contamination
2	1 ≤ CF < 3	Moderate contamination
1	CF < 1	No contamination

- **Polymetallic Contamination Degree (CD)**

This index is derived from the determination of contamination factors. It is used to estimate the polymetallic, in advance, for each sampling site. For a given site, the CD is the sum of the CFi of the n chemical elements at that site. It is calculated using the following equation:

$$CD = CF1 + CF2 + \ldots + CFn \quad (5)$$

For the interpretation of CD values, Hänkanson proposed 04 classes defined in Table 5.

- **Ecological risk index (Eri)**

This index determines the ecological sensitivity and toxicity of pollutants [25] [26]. It has been calculated specifically for arsenic and chromium. It is calculated by the following formula:

$$Eri = Tri \times CFi \quad (6)$$

- CFi: contamination factor of component i;
- Tri: toxic response factor of a given component. The Tri values used are 10

(As), 5 (Cu) 2 (Cr) and 1 (Zn) [25] [26].

For the interpretation of Eri values, Hankanson proposed 05 classes defined in Table 6.

Table 5. Interpretation of CD values.

Class	Value	Interpretation
4	CD ≥ 32	Very high contamination
3	16 ≤ CD < 32	High contamination
2	8 ≤ CD < 16	Moderate contamination
1	CD < 8	No contamination

Table 6. Interpretation of Eri values

Class	Value	Interpretation
5	Eri ≥ 320	Very high ecological risk
4	160 ≤ Eri <320	High ecological risk
3	80 ≤ Eri <160	Considerable ecological risk
2	40 ≤ Eri <80	Moderate ecological risk
1	Eri <40	Low ecological risk

- **Potential Ecological Risk Index (RI)**

This index takes into account the combined effect of several parameters, namely the toxic level, the concentration of heavy metals and the ecological sensitivity of biological communities to heavy metals [27]. The RI is calculated using the following equation:

$$RI = \sum_{i=1}^{n} Eri \tag{7}$$

where "Eri" represents the ecological risk index specific to metal *i*.

For the interpretation of Eri values, Singh proposed 05 classes defined in Table 7.

Table 7. Interpretation of RI values.

Class	Value	Interpretation
5	RI ≥ 600	Serious ecological pollution level
4	300 ≤ RI <600	Severe ecological pollution level
3	150 ≤ RI <300	Moderate ecological pollution level
1	RI <150	Low ecological pollution level

3.2.6. MTE Classification by Order of Preponderance and by Index

The following parameters were used to achieve a relative classification between TMEs:

- the average content of each ETM across all sites;
- the maximum values of three (03) indexes, Igeo, EF and CF, per TME.

For the classification of sites by contamination level, the polymetallic contamination degree (CD) has been used.

4. Results and Discussion

4.1. Sampling

As indicated above, a total of twenty (20) mining sites in the study area were subject to composite sampling (ore extraction and processing zones). Most of the processing areas are located near water sources, but for safety reasons they are also located in villages. Figure 2 shows the mappable localities hosting the mining sites in the study area.

4.2. XRF Spectrometry Analysis

The results of the XRF analysis are presented in Table 8.

4.3. Statistical Analysis of XRF Results

- **Monovariate statistics**

  Table 9 shows the statistical parameters for the six (06) MTEs that met the

Table 8. XRF analysis results (ppm).

N°	Mine sites	UTM Coordinates		Chemical components						
		X	Y	As	Zn	Cu	Ni	Cr	V	Ti*
1	Alékran	212112.07	767744.12	24.18	65.66	98.05	115.85	377.55	378.77	7109.23
2	Aley	222905.91	770538.91	11.68	69.63	125.85	184.45	423.66	343.18	6872.94
3	Allaiyaokro	223964	773501.55	11.32	53.50	39.41	55.55	209.06	161.73	6577.91
4	Angovia	219116	776772.02	70.07	60.37	116.16	102.26	459.49	330.42	4400.53
5	Benou	217715.99	788278.99	30.93	42.22	73.42	84.85	185.53	273.90	5304.00
6	Bozi	220990.97	765411.98	10.94	64.26	59.85	78.43	256.35	210.31	3978.21
7	Degbezre	206335.99	774229.02	31.83	60.97	123.22	127.32	452.93	442.12	5560.13
8	Kaviéssou	207509.41	766151.15	23.63	48.68	136.71	103.18	442.48	401.53	6259.47
9	Kouassi Périta	207215.24	768370.4	28.18	62.23	108.54	119.16	365.13	386.02	7470.31
10	Koudougou	205963.95	767576.93	31.77	52.71	109.09	133.52	389.26	314.53	9334.52
11	Krigambo	187757.13	784390.98	8.51	71.93	34.05	60.94	311.16	213.54	3375.99
12	Ndenou	207743	775520.01	45.22	91.44	104.23	123.87	545.27	491.45	6570.44
13	Ouanzanou	208423.99	773823.99	47.10	45.96	120.15	94.73	426.75	380.53	5737.74
14	Bel Chantier	199048.21	804717.55	4.29	61.41	19.86	42.61	184.40	104.68	4013.69
15	Lagrikro	201303.87	802530.14	10.84	34.24	37.39	71.08	286.98	174.18	5498.74
16	Okabo	201227.92	803692.03	4.94	91.81	59.32	131.44	243.57	144.27	3332.02
17	Pakouabo	193681.88	792739.05	8.13	21.70	38.31	44.55	215.67	161.92	5906.94
18	Kouakougnanou	221979	775864	11.16	69.61	74.35	99.96	189.62	186.28	5033.75
19	Toumbokro	223485.15	768040.93	4.80	84.15	106.48	149.56	344.43	190.56	4226.40
20	Zagouta	213279	766340.94	72.13	86.87	122.85	182.92	677.74	496.90	5608.70
UCC contents (ppm)				**2**	**52**	**14.3**	**18.6**	**35**	**53**	**3117**

*Normalising element for calculating the enrichment factor.

Table 9. Descriptive statistics (quantitative data).

	As	Zn	Cu	Ni	Cr	V
No. of observations	20	20	20	20	20	20
Minimum	4.29	21.70	19.86	42.61	184.40	104.68
Maximum	72.13	91.81	136.71	184.45	677.74	496.90
Median	17.66	61.82	101.14	102.72	354.78	294.22
Medium (M)	24.58	61.97	85.36	105.31	349.35	289.34
Variance (n − 1)	422.99	341.12	1393.66	1652.14	17590.82	14961.98
Standard deviation (n − 1)	20.57	18.47	37.33	40.65	132.63	122.32
UCC (ppm)	2.00	52.00	14.30	18.60	35.00	53.00
M/UCC	**12.29**	**1.19**	**5.97**	**5.66**	**9.98**	**5.46**

selection criteria after XRF analysis, namely abundance, complete detection at all sites and proven toxicity naturally or by accumulation in receiving environments.

The ratio of crustal mean and abundance (M/UCC) is greater than 1 for the six (06) TMEs analyzed, indicating enrichment in these elements [28].

- **Multivariate statistics**

The following table shows the results of linear relationships between MTEs, based on Pearson correlation coefficients. Values in bold indicate a significant correlation. This matrix shows some pairs of elements with correlations ranging from strong to very strong (Pearson classification; Table 10).

✧ For very strong correlations, we have the following two (02) MTE pairs: Cu_V: 0.831 and Cr_V: 0.883;

✧ For high intensity correlations, we have: As_Cr: 0.769; As_V: 0.759; Cu_Ni: 0.772; Cu_Cr: 0.773 and, to a lesser degree, As_Cu: 0.618; Ni_Cr: 0.689 and Ni_Cr: 0.603.

This finding is confirmed by the Principal Component Analysis (PCA) and the scree plot (or cone diagram; Figure 4) below represented from the eigenvalues (Table 11) which indicate the following 02 components: Component 1: As, Cu, Cr and V; Component 2: Zn and Ni.

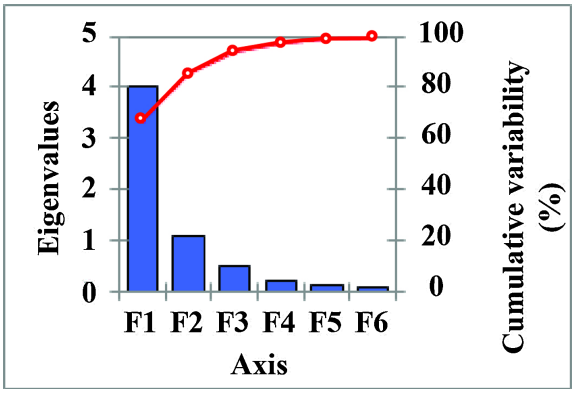

Figure 4. Scree plot.

Table 10. Correlation matrix (Pearson (n − 1)).

Variables	As	Zn	Cu	Ni	Cr	V
As	**1**					
Zn	0.128	**1**				
Cu	0.618	0.247	**1**			
Ni	0.385	0.597	**0.772**	**1**		
Cr	**0.769**	0.388	**0.773**	0.689	**1**	
V	**0.759**	0.234	**0.831**	0.603	**0.883**	**1**

Table 11. Eigenvalues.

	F1	F2	F3	F4	F5	F6
Eigenvalues	4.021	1.104	0.486	0.190	0.132	0.067
Variability (%)	67.018	18.399	8.097	3.169	2.193	1.123
% cumulative	67.018	85.417	93.514	96.684	98.877	100.000

The PCA carried out enabled us to visualize the variables, *i.e.* the MTEs targeted by the study, as well as the mining sites concerned as shown in Figures 5-7.

On these representations, we can see that the MTEs are well represented on the correlation circle (far from the center). Their relationships with the mining localities are described as follows:

- ✧ Angovia, Ouanzanou, Kaviessou, Degbezre, Kouassi Perita and Koudougou are rich in As, Cr, V and Cu;
- ✧ N'Denou, Zagouta, Alekran and Aley are moderately rich in all MTEs;

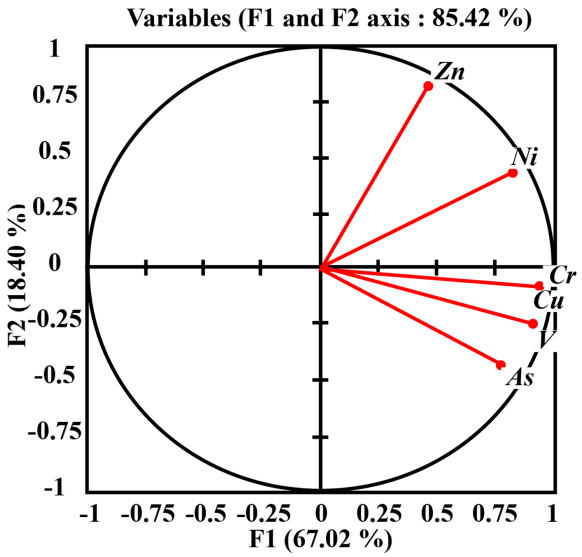

Figure 5. Correlation circle of variables (TMEs).

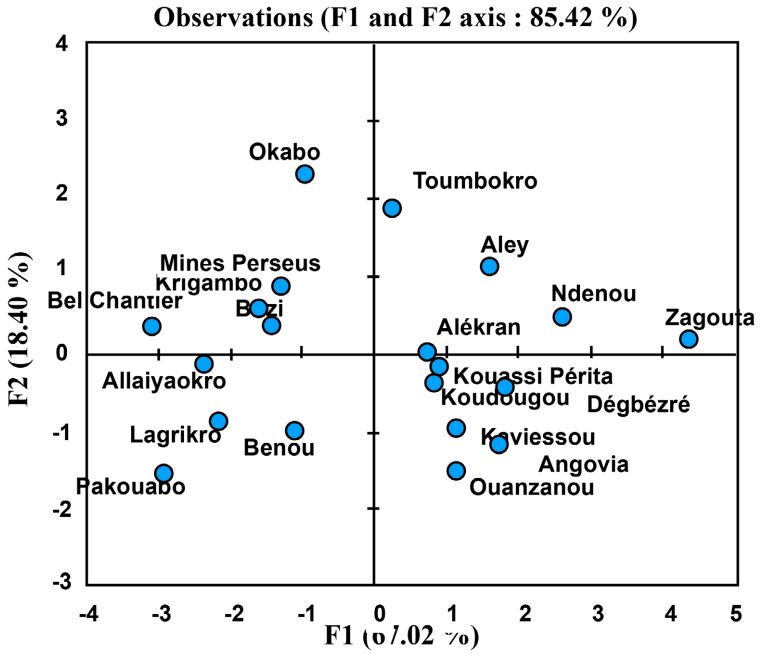

Figure 6. Observations graph of mining sites.

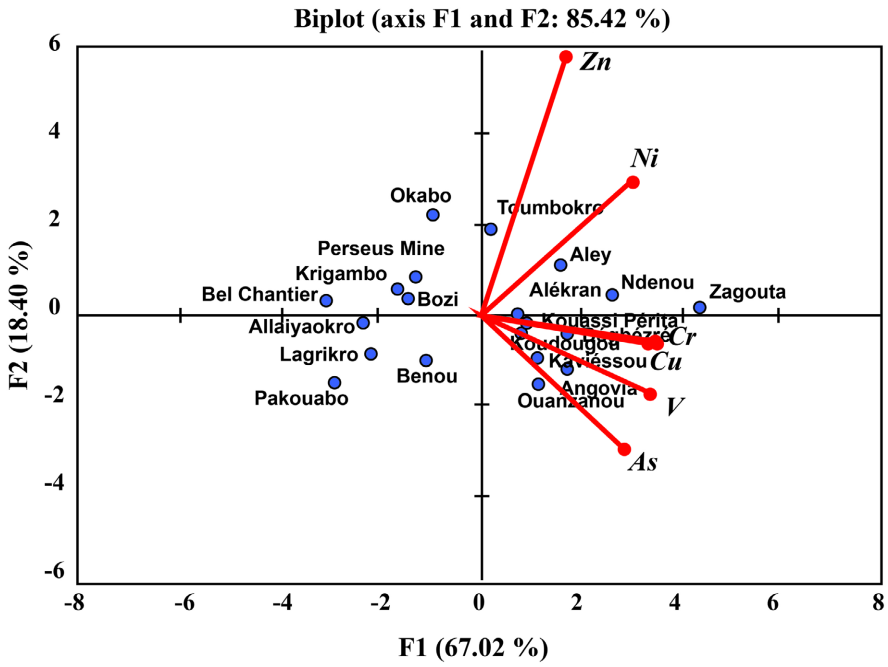

Figure 7. Graph showing MTEs and mine sites.

- ✧ Toumbokro correlates well with the vertical axis and is richer in Zn and Ni;
- ✧ The other localities to the left of the vertical axis are relatively poor in all the MTEs studied.

4.4. Index calculations

Table 12 shows the results of Igeo and EF calculations for each site.

Table 12. Geoaccumulation index and enrichment factors.

		Igeo						EF					
N°	Mine sites	As	Zn	Cu	Ni	Cr	V	As	Zn	Cu	Ni	Cr	V
1	Alékran	3.01	−0.25	2.19	2.05	2.85	2.25	5.30	0.55	3.01	2.73	4.73	3.13
2	Aley	1.96	−0.16	2.55	2.72	3.01	2.11	2.65	0.61	3.99	4.50	5.49	2.94
3	Allaiyaokro	1.92	−0.54	0.88	0.99	1.99	1.02	2.68	0.49	1.31	1.42	2.83	1.45
4	Angovia	4.55	−0.37	2.44	1.87	3.13	2.06	24.82	0.82	5.75	3.89	9.30	4.42
5	Benou	3.37	−0.89	1.78	1.60	1.82	1.78	9.09	0.48	3.02	2.68	3.12	3.04
6	Bozi	1.87	−0.28	1.48	1.49	2.29	1.40	4.29	0.97	3.28	3.30	5.74	3.11
7	Degbezre	3.41	−0.36	2.52	2.19	3.11	2.48	8.92	0.66	4.83	3.84	7.25	4.68
8	Kaviéssou	2.98	−0.68	2.67	1.89	3.08	2.34	5.88	0.47	4.76	2.76	6.30	3.77
9	Kouassi Périta	3.23	−0.33	2.34	2.09	2.80	2.28	5.88	0.50	3.17	2.67	4.35	3.04
10	Koudougou	3.40	−0.57	2.35	2.26	2.89	1.98	5.30	0.34	2.55	2.40	3.71	1.98
11	Krigambo	1.50	−0.12	0.67	1.13	2.57	1.43	3.93	1.28	2.20	3.03	8.21	3.72
12	Ndenou	3.91	0.23	2.28	2.15	3.38	2.63	10.73	0.83	3.46	3.16	7.39	4.40
13	Ouanzanou	3.97	−0.76	2.49	1.76	3.02	2.26	12.79	0.48	4.56	2.77	6.62	3.90
14	Bel Chantier	0.52	−0.35	−0.11	0.61	1.81	0.40	1.67	0.92	1.08	1.78	4.09	1.53
15	Lagrikro	1.85	−1.19	0.80	1.35	2.45	1.13	3.07	0.37	1.48	2.17	4.65	1.86
16	Okabo	0.72	0.24	1.47	2.24	2.21	0.86	2.31	1.65	3.88	6.61	6.51	2.55
17	Pakouabo	1.44	−1.85	0.84	0.68	2.04	1.03	2.15	0.22	1.41	1.26	3.25	1.61
18	Kouakougnanou	1.90	−0.16	1.79	1.84	1.85	1.23	3.46	0.83	3.22	3.33	3.35	2.18
19	Toumbokro	0.68	0.11	2.31	2.42	2.71	1.26	1.77	1.19	5.49	5.93	7.26	2.65
20	Zagouta	4.59	0.16	2.52	2.71	3.69	2.64	20.04	0.93	4.77	5.47	10.76	5.21

Igeo value interpretation [21]

Class	Value	Interpretation
7	Igeo ≥ 5	Extremely polluted
6	4 ≤ Igeo < 5	From heavily polluted to extremely polluted
5	3 ≤ Igeo < 4	Heavily polluted
4	2 ≤ Igeo < 3	From Moderately to heavily polluted
3	1 ≤ Igeo < 2	Moderately polluted
2	0 ≤ Igeo < 1	From unpolluted to moderately polluted
1	Igeo < 0	unpolluted

EF value interpretation [23]

Class	Value	Interpretation
5	EF ≥ 40	Extreme enrichment
4	20 ≤ EF < 40	Moderately severe enrichment
3	5 ≤ EF < 20	Moderate enrichment
2	2 ≤ EF < 5	Minor enrichment
1	EF < 2	No enrichment

The Igeo table shows that all sites are polluted with at least four (04) TMEs, notably, As, Cr, Ni, Cu and V. Igeo values range from 0.52 to 4.59 (As), −1.85 to 0.24 (Zn), −0.11 to 2.67 (Cu), 0.61 to 2.72 (Ni), 1.81 to 3.69 (Cr) and 0.40 to 2.64

(V). The Igeo is therefore more pronounced for As and Cr, in contrast to Zn, whose Igeo is below zero at almost all sites. The same trend is observed for the Enrichment Factor, where As and Cr are still the most pronounced at almost all sites. Values range from 1.67 to 24.82 (As), 0.22 to 1.65 (Zn), 1.08 to 5.75 (Cu), 1.26 to 6.61 (Ni), 2.83 to 10.76 (Cr) and 1.45 to 5.21 (V).

- **Contamination Facteur (CF), polymetallic contamination degree (CD) and ecological risk parameters**

According to [29], a distinction must be made between contamination, which is the introduction of "a potentially dangerous substance, whatever its content" into the natural transfer and exposure media of soil, air and water, and pollution, which is present when "the content is potentially dangerous or reaches the limit values set by standards". Contamination is therefore not synonymous with pollution. Table 13 shows the results of the CF and CD.

Table 13. Factors and degrees of contamination/ecological risk parameters.

CONTAMINATION FACTOR (CF)									ECOLOGICAL RISK PARAMETERS		
		CF						CD	Eri_As-Cr		RI_As-Cr
N°	Mine sites	As	Zn	Cu	Ni	Cr	V		As	Cr	
1	Alékran	12.09	1.26	6.86	6.23	10.79	7.15	44.37	120.92	10.79	131.70
2	Aley	5.84	1.34	8.80	9.92	12.10	6.48	44.48	58.4	12.10	70.50
3	Allaiyaokro	5.66	1.03	2.76	2.99	5.97	3.05	21.46	56.6	5.97	62.57
4	Angovia	35.04	1.16	8.12	5.50	13.13	6.23	69.18	350.36	13.13	363.49
5	Benou	15.47	0.81	5.13	4.56	5.30	5.17	36.44	154.65	5.30	159.95
6	Bozi	5.47	1.24	4.19	4.22	7.32	3.97	26.40	54.72	7.32	62.04
7	Degbezre	15.92	1.17	8.62	6.85	12.94	8.34	53.83	159.15	12.94	172.09
8	Kaviéssou	11.82	0.94	9.56	5.55	12.64	7.58	48.08	118.16	12.64	130.80
9	Kouassi Périta	14.09	1.20	7.59	6.41	10.43	7.28	47.00	140.9	10.43	151.33
10	Koudougou	15.89	1.01	7.63	7.18	11.12	5.93	48.76	158.85	11.12	169.97
11	Krigambo	4.26	1.38	2.38	3.28	8.89	4.03	24.22	42.55	8.89	51.44
12	Ndenou	22.61	1.76	7.29	6.66	15.58	9.27	63.17	226.1	15.58	241.68
13	Ouanzanou	23.55	0.88	8.40	5.09	12.19	7.18	57.30	235.49	12.19	247.68
14	Bel Chantier	2.15	1.18	1.39	2.29	5.27	1.98	14.25	21.45	5.27	26.72
15	Lagrikro	5.42	0.66	2.61	3.82	8.20	3.29	24.00	54.2	8.20	62.40
16	Okabo	2.47	1.77	4.15	7.07	6.96	2.72	25.13	24.7	6.96	31.66
17	Pakouabo	4.07	0.42	2.68	2.40	6.16	3.06	18.77	40.65	6.16	46.81
18	Kouakougnanou	5.58	1.34	5.20	5.37	5.42	3.51	26.42	55.8	5.42	61.22
19	Toumbokro	2.40	1.62	7.45	8.04	9.84	3.60	32.94	24	9.84	33.84
20	Zagouta	36.07	1.67	8.59	9.83	19.36	9.38	84.90	360.65	19.36	380.01

Class	CF value interpretation	
4	CF ≥ 6	Very high contamination
3	3 ≤ CF < 6	High contamination
2	1 ≤ CF < 3	Moderate contamination
1	CF < 1	No contamination

Class	CD value interpretation	
4	CD ≥ 32	Very high contamination
3	16 ≤ CD < 32	High contamination
2	8 ≤ CD < 16	Moderate contamination
1	CD < 8	No contamination

Class	Eri value interpretation	
5	**Eri ≥ 320**	Very high ecological risk
4	**160 ≤ Eri < 320**	High ecological risk
3	**80 ≤ Eri < 160**	Considerable ecological risk
2	**40 ≤ Eri < 80**	Moderate ecological risk
1	**Eri < 40**	Low ecological risk

Class	RI value interpretation	
4	RI ≥ 600	Serious ecological pollution level
3	300 ≤ RI < 600	Severe ecological pollution level
2	150 ≤ RI < 300	Moderate ecological pollution level
1	RI < 150	Low ecological pollution level

calculations for each site and for the targeted chemical elements. It should be remembered that the results of the Igeo and EF calculations enabled us to distinguish As and Cr as major pollutants. The eventual solubilization of these two (02) TMEs and their accumulation in receiving environments such as water can affect the food chain. For this reason, ecological risk parameters for these two (02) ETMs were also calculated.

A look at the coloring of the tables in relation to contamination/pollution intensities provides information on the severity of the sites' situation, except for zinc contamination, where CF values range from 0.42 to 1.77. The CF values for the other TMEs range from 2.15 to 36.07 (As), 1.39 to 9.56 (Cu), 2.29 to 9.92 (Ni), 5.27 to 19.36 (Cr) and 1.98 to 9.38 (V).

4.5. TMEs Classification

4.5.1. Classification of TMEs in Order of Preponderance and by Index

The approach adopted for the relative classification of the MEs targeted has enabled us to determine the preponderance levels in Table 14. This table takes into account the average content of each TME across all sites and the maximum values of three (03) indices, Igeo, EF and CF per TME.

Table 14. TMEs preponderance table.

TME	Average content on sites (ppm)	UCC content (ppm)	Max. Igeo	Max. EF	Max. CF
As	24.5	2	4.59	24.82	36.07
Zn	61.97	52	0.24	1.65	1.76
Cu	85.36	14.3	2.67	5.75	9.56
Ni	105.31	18.6	2.72	6.61	9.92
Cr	349.35	35	3.69	10.76	19.36
V	289.34	53	2.64	5.21	9.38

The following classifications emerge from these graphs (Figure 8 and Figure 9):

- For average grades, it can be seen that all grades at the sites are well above those of the upper continental crust. The preponderance of TMEs on the basis of average grades leads to the following classification: Cr (349.35) > V (289.34) > Ni (105.31) > Cu (85.36) > Zn (61.97) > As (24.5).
- For indexes, the maximum values allow the following classification of contamination/pollution levels:
- Igeo: As (4.59) > Cr (3.69) > Ni (2.72) > Cu (2.67) > V(2.64) > Zn (0.24);
- EF: As (24.82) > Cr (10.76) > Ni (6.61) > Cu (5.75) > V(5.21) > Zn (1.65);
- CF: As (36.07) > Cr (19.36) > Ni (9.92) > Cu (9.56) > V(9.38) > Zn (1.76).

Arsenic and chromium are therefore the dominant TMEs and the main contaminants and/or pollutants in the study area.

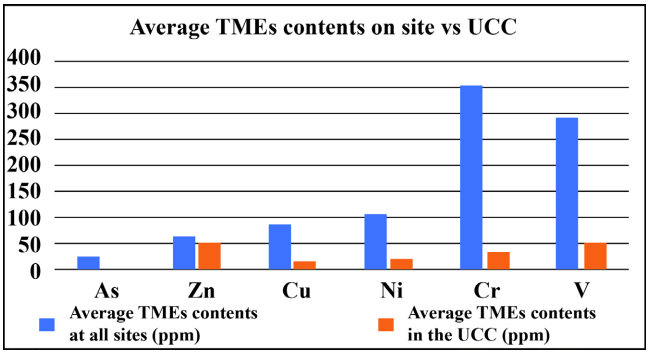

Figure 8. TMEs classification based on average levels at sites/UCC.

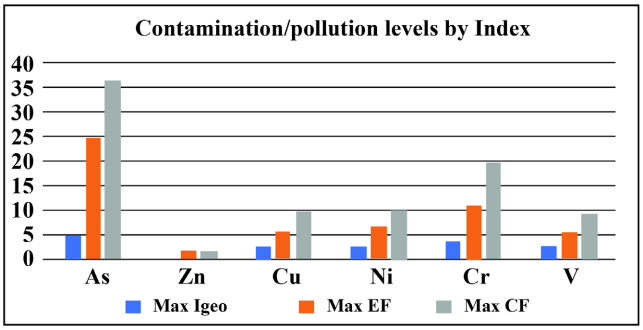

Figure 9. Classification of TME contamination/pollution levels by index.

4.5.2. Classification of Contamination/Pollution Levels by Locality

The classification of contamination/pollution levels by locality is based on potential ecological risk indices, specifically for arsenic and chromium, which are the most abundant, and degrees of contamination. The results are shown in Figure 10 and Figure 11.

The graphs showing the classification of contamination or pollution levels by locality illustrate the extent of the adverse effects of mining activities throughout the study area.

- Twelve (12) of the twenty (20) localities are very heavily contaminated (CD >

32) (Figure 10). These are, in descending order, Zagouta, Angovia, N'Denou, Ouanzanou, Dégbezre, Kaviessou, Koudougou, Kouassi Perita, Alékran, Aley, Benou and Toumbokro;

- Two (02) localities have a high potential ecological risk level (300 ≤ RI < 600) in As and Cr (Figure 11). These are Zagouta and Angovia;
- Six (06) localities (apart from the two mentioned) have a moderate level of potential ecological risk (150 ≤ RI < 300). These are, in descending order, Ouanzanou, N'Denou, Koudougou, Dégbezre, Benou and Kouassi Perita.

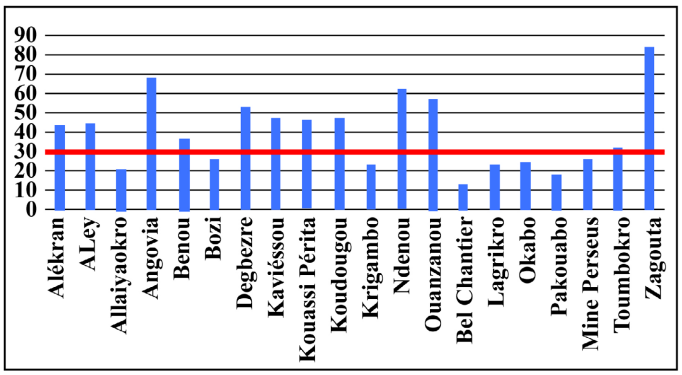

Figure 10. CDs classification by locality.

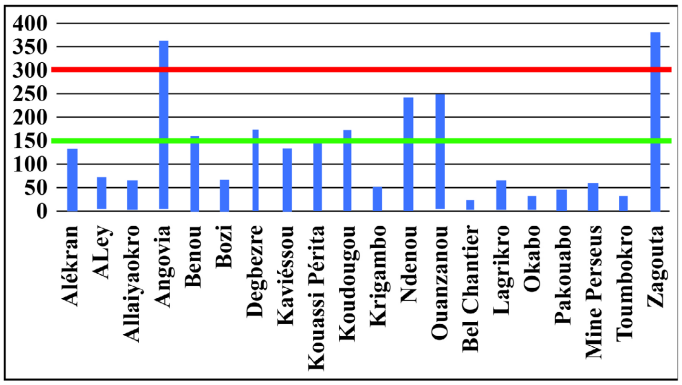

Figure 11. Classification of arsenic and chromium RI by locality.

It should be pointed out that these localities are all located at the foot of the Yaoure Mountains. Angovia and Zagouta, the localities of greatest concern, are former gold-panning sites that are still active. The same applies to Kaviéssou, Alékran, Aley, Toumbokro and Kouassi Périta. On the other hand, the N'Denou, Benou and Dégbézré sites are recent but very active. All these sites require environmental monitoring.

4.6. Results of XRD Analysis

4.6.1. Diffractograms Analysis

The analysis of ten (10) samples consisting of clays, saprolites, slightly altered rocks and sludges yielded the following diffractograms.

By interpreting the results of the XRD analyses, it is possible to identify the

minerals that make up the various samples (Table 15). Dominant minerals are shown in bold.

Table 15. XRD results for samples.

Id.	Localization	Type	Minerals
D01	*Zagouta* (ou Zegata)	Argile	**Pyrrhotite**, Filipstadite, Amesite, Tugtupite, Ulvospinel, Stenhuggarite
D02	*Ouanzanou*	Argile	**Perryite**, Periclase, Eucryptite, Stenhuggarite, Tulameenite, Bowieite, Kesterite
D03	*N'Denou*	Argile	**Periclase**, Calcite, Stenhuggarite, Filipstadite, Wuestite, Tanteuxenite-(Ho),Roaldite
D04	Kouakougnanou	Saprock	**Filipstadite**, Chlorure de fer, Siderite, Periclase, Villiaumite, Calcite
D05	*Angovia*	Saprock	**Antigorite**, Stenhuggarite, Polkanovite, Filipstadite, Deerite, Perkovaite, Tanteuxenite (Lu),
D06	Kaviessou	Saprolite	**Periclase**, Pentlandite, Carlinite, Stenhuggarite, Tanteuxenite-(Yb), Bredigite
D07	Aley	Saprock	**Carlinite**, Calcite, Stenhuggarite, Chloritoide, Periclase, Ixiolite, Braunite
D08	*Kouassi Perita*	Saprolite	**Calcite**, Filipstadite, Anatase, Perovskite, Carlinite, Nitratine
D09	*Degbezre*	Boue	**Carlinite**, Cavoite, Periclase, Eucryptite, Dolomite, Stenhuggarite, Manganosite, Nitratine
D10	Alékran	Boue	**Stenhuggarite**, Carlinite, Tanteuxenite-(Ho), Calcite, Filipstadite, Ferrocolumbite

XRD analysis of the samples clearly shows that the mineralogy of the samples is complex but mainly dominated by stenhuggarite ($CaFe^{3+}(As^{3+}O_2)(As^{3+}SbO_5)$), periclase (MgO), pyrrhotite ($Fe_{1-x}S$ (where x varies from 0 to 0.20), carlinite (TI_2S), filipstadite ($(Mn,Mg)(Sb^{5+}_{0.5}\ Fe^{3+}_{0.5})O_4$), calcite ($CaCO_3$) and Antigorite ($(Mg, Fe\ II)_3\ Si_2O_5\ (OH)_4$)).

The elements Fe, Mg and Si are not too problematic for the environment, but sulfide minerals such as pyrrhotite are potentially acidogenic and arsenates, potentially toxic. It should be noted that the base rocks contain carbonates (calcite and dolomites) that can act as neutralizers in the event of Acid Mine Drainage (AMD) [30].

4.6.2. Possible Sources of Contaminants

As mentioned above, the geology of the Yaouré furrow is made up of an assemblage of magmatic volcanic, intrusive and sedimentary rocks. Most of the mining sites incriminated by potential ecological risks and/or high levels of contamination are located in the following lithological formations (Figure 11):

- Basaltic volcanoclastites and metavolcanites: Angovia and Zagouta (or Zegata) (granite-volcanite contact zones);
- Sandstones changing to argillites: N'Denou, Ouanzanou, Degbezre, Kouassi Perita and Kaviessou;
- Sandstone, conglomerates: Benou.

It should be noted that a study by [6] showed that the metalliferous paragenesis in the Yaoure furrow is mainly represented by pyrite (abundant) and chalcopyrite (frequent). The presence of pyrrhotite, pentlandite and magnetite, as well as traces of sphalerite, cubanite, bravoite, lineite, molybdenite, Bi, Ni, Hg tellurides (tetradymite, melonite, coloradoite) and cassiterite was reported by [31].

Their work also showed that Angovia's gold mineralization is linked to intense hydrothermal alteration with quartz, chlorite, carbonates and sulfides.

Among other phenomena, this hydrothermal alteration led to corrosion of the sulfides, the mineral carriers of the contaminants studied. This corrosion was followed by soil reworking due to intensive mining activity in the area, as demonstrated by the high levels of enrichment factors in several localities. Chromium and vanadium may also have originated from ultrabasic rocks reported in the study area.

4.6.3. Implications of the Study for Human Health and the Food Chain

The risk of a chemical element's impact on the environment depends on its pollutant capacity, linked to its concentration and reactivity, which in turn depends on several parameters, including its chemical form and mobility in the environment. Here we provide some informations on chromium and arsenic, the main pollutants in the study area.

- Arsenic occurs naturally in the environment, and everyone is slightly exposed to it. Food and water account for most of the total daily dose of arsenic adsorbed by ingestion. In the case of arsenic-polluted sites and soils, the main risks are pollution of the underlying groundwater. Risks from other exposure routes are less significant [32]. Its maximum permissible concentration in water intended for human consumption has been set at 10 µg/L, according to World Health Organization (WHO) recommendations. Inorganic arsenic (in pure form or bound to oxygen, chlorine or sulfur), as found on mining sites, is far more toxic than organic arsenic (bound to carbon or hydrogen);
- Chromium occurs naturally in small quantities in all types of rock and soil. The toxicity of chromium varies greatly according to its chemical form. According to the International Agency for Research on Cancer (IARC), chromium VI is carcinogenic and can be bioaccumulated by various organisms. It is the most mobile form of chromium in terrestrial and aquatic environments.

5. Conclusions

The assessment of metal contamination shows that four (04) of the six (06) TMEs studied, chromium, arsenic, vanadium and copper, have high correlations and form the majority of the principal component in the multivariate statistical analysis. As for the various contamination or pollution indices (Igeo, EF, CF and CD), the values obtained rank chromium and arsenic as the main TMEs with high levels, capable of posing major environmental problems, especially in aquatic environments. These TMEs are potentially dangerous pollutants, and their management is essential to protect human health and the environment. There are a great many processes for treating metal-polluted soils, but very few are actually applied. Those that seem to be most widely used are: containment - solidification/stabilization - landfilling - washing - or combinations of these processes [32].

As part of this study, we are proposing phytoremediation, an effective and

economical technique for renaturating polluted sites while preserving the soil's properties (fertility). Phytoremediation is a soil, water and even air decontamination technique that uses the natural capacities of plants to eliminate or reduce the concentration of pollutants. It can be used alone or in combination with other remediation techniques such as bioremediation and green chemistry. Phytoremediation projects using fast-growing local plants are currently being tested on mining sites in the Tengrela region of northern Côte d'Ivoire, by the Côte d'Ivoire Mining Development Company (SODEMI) in collaboration with private partners. If the results are convincing, this experiment should be extended to all mining sites located in the Birimian area of Côte d'Ivoire and West Africa, where the majority of gold mining activities are concentrated. A more in-depth study needs to be carried out, focusing in particular on the analysis of As and Cr concentrations in water, sediments and fishery products and, in the event of proven occurrence, on their speciation.

Acknowledgements

We would like to thank the "Institut de Recherche pour le Développement (IRD)" and the "ACE Partners" sustainable mining network for funding my research. We would also like to thank the actors of the "Centre d'Excellence Africain Mines et Environnement Minier (CEA-MEM)" for all the material assistance they provided during my work.

Conflicts of Interest

The authors declare no conflicts of interest regarding the publication of this paper.

References

[1] Chon, H., Kim, K. and Kim, J. (1995) Metal Contamination of Soils and Dusts in Seoul Metropolitan City, Korea. *Environmental Geochemistry and Health*, **17**, 139-146. https://doi.org/10.1007/bf00126082

[2] Rybicka, E.H. and Jedrzejczyk, B. (1995) Preliminary Studies on Mobilisation of Copper and Lead from Contaminated Soils and Readsorption on Competing Sorbents. *Applied Clay Science*, **10**, 259-268. https://doi.org/10.1016/0169-1317(95)00006-p

[3] Lee, C.G., Chon, H. and Jung, M.C. (2001) Heavy Metal Contamination in the Vicinity of the Daduk Au-Ag-Pb-Zn Mine in Korea. *Applied Geochemistry*, **16**, 1377-1386. https://doi.org/10.1016/s0883-2927(01)00038-5

[4] Leila, S., Hadef El Okki, M.E., Fatima-Zorhra, A.M. and Smail, M. (2014) Utilisation d'indices pour l'évaluation de la qualité des sédiments: Cas du bassin de Boumerzoug (Algérie). *European Scientific Journal*, **10**, 333-343.

[5] Smouni, A., Ater, M., Auguy, F., Laplaze, L., Mzibri, M.E., Berhada, F., *et al.* (2010) Évaluation de la contamination par les éléments-traces métalliques dans une zone minière du Maroc oriental. *Cahiers Agricultures*, **19**, 273-279. https://doi.org/10.1684/agr.2010.0413

[6] Coulibaly, Y., Kouamelan, A.N., Djro, C.S., Pothin, K.B.K. and Boffoué, M.O.

(2008) Les altérations associées à la minéralisation aurifère d'Angovia (massif du Yaouré, Centre de la Côte d'Ivoire). *Revue Ivoirienne des Sciences et Technologie*, **11**, 159-175.

[7] Diarra, Y., Ouattara, G., Barthélémy Gnammytchet Koffi, G.B. and Yao, K.A. (2018) Prédiction du drainage minier acide et modélisation environnementale à partir des caractéristiques géologiques intrinsèques du gisement aurifère de Sissingué, Nord de la Côte d'Ivoire. *Afrique SCIENCE*, **14**, 94-106.

[8] Bessoles, B. (1977) Géologie de l'Afrique-Le craton Ouest Africain. Mémoires BRGM, 88 Paris.

[9] Abouchami, W., Boher, M., Michard, A. and Albarede, F. (1990) A Major 2.1 Ga Event of Mafic Magmatism in West Africa: An Early Stage of Crustal Accretion. *Journal of Geophysical Research: Solid Earth*, **95**, 17605-17629. https://doi.org/10.1029/jb095ib11p17605

[10] Pouclet, A., Vidal, M., Delor, C., Siméon, Y. and Alric, G. (1996) Le volcanisme birimien du nord-est de la Côte d'Ivoire, mise en évidence de deux phases volcano-tectoniques distinctes dans l'évolution géodynamique du Paléoprotérozoïque. *Bulletin de la Société Géologique de France*, **167**, 529-541.

[11] Vidal, M., Delor, C., Pouclet, A., Simeon, Y. and Alric, G. (1996) Evolution géodynamique de l'Afrique entre 2, 2 et 2 Ga: le style "archéen" des ceintures vertes et des ensembles sédimentaires birimiens du nord-est de la Côte d'Ivoire. *Bulletin de la Société Géologique de France*, **167**, 307-319.

[12] Vidal, M., Gumiaux, C., Cagnard, F., Pouclet, A., Ouattara, G. and Pichon, M. (2009) Evolution of a Paleoproterozoic "Weak Type" Orogeny in the West African Craton (Ivory Coast). *Tectonophysics*, **477**, 145-159. https://doi.org/10.1016/j.tecto.2009.02.010

[13] Fabre, R., Ledru, P. and Milesi, J.P. (1990) Le Protérozoïque inférieur (Birrimien) du centre de la Côte d'Ivoire, évolution tectonique et corrélations. *Comptes Rendus de l'Académie des Sciences*, **311**, 971-976.

[14] Feybesse, J. and Milési, J. (1994) The Archaean/Proterozoic Contact Zone in West Africa: A Mountain Belt of Décollement Thrusting and Folding on a Continental Margin Related to 2.1 Ga Convergence of Archaean Cratons? *Precambrian Research*, **69**, 199-227. https://doi.org/10.1016/0301-9268(94)90087-6

[15] Delor, C., Siméon, Y., Vidal, M., Zeade, Z., Koné, Y., Adou, M., Dibouahi Irié, D.B., Ya, B.D., N'da, D., Pouclet, A., Konan, G., Diaby, I., Chiron, J.C., Dommanget, A., Kouamelan, A.N., Peucat, J.J., Cocherie, A. and Cautru, J.P. (1995) Carte géologique de la Côte d'Ivoire à 1/200 000, feuille Gagnoa. Direction des Mines et de la Géologie, Abidjan-Côte d'Ivoire.

[16] Thermo Fisher Scientific Inc. (2008) On-Site Elemental Analysis of Art and Artifacts. Art Conservation and Archaeometric Studies with Thermo Scientific Niton XL3t Series Handheld XRF Analyzers. https://www.thermofisher.com/document-connect/document-connect.html?url=https://assets.thermofisher.com/TFS-Assets%2FCAD%2FApplication-Notes%2FArt-Artifacts.pdf

[17] Technical Report Yaouré Gold Project Côte d'Ivoire (2017) Perseus Mining Limited. 294. https://perseusmining.com/wp-content/uploads/2021/09/20171218_Yaoure_NI43-101.pdf

[18] Hans Wedepohl, K. (1995) The Composition of the Continental Crust. *Geochimica et Cosmochimica Acta*, **59**, 1217-1232.

https://doi.org/10.1016/0016-7037(95)00038-2

[19] Jean-Gael, I.B.T. (2017) Caractérisation de l'Interface eau-sédiment dans un environnement lagunaire à forçage: Hydrologie et évaluation environnementale du chenal est de la lagune Ebrié (côte d'Ivoire). Thèse unique, Université Félix Houphouët-Boigny.

[20] Baize, D. (2009) Éléments traces dans les sols. Fonds géochimiques, fonds pédogéochimiques naturels et teneurs agricoles habituelles: Définitions et utilités. *Courrier de l'Environnement de l'INRA*, **57**, 63-72.

[21] Müller, G. (1981) Die schwermetallbelastung der sedimente des neckars und seiner Nebenflusse: Eine Bestandsaufnahme. *Chemical Zeitung*, **105**, 157-164.

[22] Lundemi, L.K., Neema, S.S., Atibu, E.K., Mulaji, C.K., Tangou, T.T., Nsimanda, C.I., *et al.* (2022) Heavy Metal Levels and Potential Ecological Risks Assessed at an Agroecosystem Site in Tropical Region. *Journal of Geoscience and Environment Protection*, **10**, 42-60. https://doi.org/10.4236/gep.2022.109003

[23] Sutherland, R.A., Tolosa, C.A., Tack, F.M.G. and Verloo, M.G. (2000) Characterization of Selected Element Concentrations and Enrichment Ratiosin Background and Anthropogenically Impacted Roadside Areas. *Archives of Environmental Contamination and Toxicology*, **38**, 428-438. https://doi.org/10.1007/s002440010057

[24] Bourdoiseau, J. and Delolme, C. (2016) Le titane dans les sédiments de l'Assainissement pluvial urbain: Sources, concentrations, mobilités. *Environnement, Ingénierie & Développement*, **71**, 35-48. https://doi.org/10.4267/dechets-sciences-techniques.3416

[25] Hakanson, L. (1980) An Ecological Risk Index for Aquatic Pollution Control. A Sedimentological Approach. *Water Research*, **14**, 975-1001. https://doi.org/10.1016/0043-1354(80)90143-8

[26] Suresh, G., Sutharsan, P., Ramasamy, V. and Venkatachalapathy, R. (2012) Assessment of Spatial Distribution and Potential Ecological Risk of the Heavy Metals in Relation to Granulometric Contents of Veeranam Lake Sediments, India. *Ecotoxicology and Environmental Safety*, **84**, 117-124. https://doi.org/10.1016/j.ecoenv.2012.06.027

[27] Singh, M., Müller, G. and Singh, I.B. (2002) Heavy Metals in Freshly Deposited Stream Sediments of Rivers Associated with Urbanisation of the Ganga Plain, India. *Water, Air, and Soil Pollution*, **141**, 35-54. https://doi.org/10.1023/a:1021339917643

[28] Rakotondramano, H., Razafindrakoto, B., Farasoa, J. and Rasolomanana, M. (2021) Analyse des données géochimiques par méthodes statistiques multivariées, cas d'exploration minière au Nord-Ouest de Madagascar. *MadaRevues*, **4**, 1-25.

[29] Jeannot, R., Lemière, B. and Chiron, S. (2001) Guide méthodologique pour l'Analyse des sols pollutes-Document du BRGM. BRGM, Orléans, 298.

[30] Diarra, Y. (2019) Prédiction du drainage minier acide à partir des caractéristiques géologiques intrinsèques d'un gisement d'or birimien: Cas du projet Sissengué, Nord de la Côte d'Ivoire. Thèse, Institut National Polytechnique Félix Houphouët-Boigny.

[31] Milesi, J.P., Feybesse J.L., Ledru, P., Dommanget, A., Ouedraogo, M.F., Marcoux, E., Prost, A., Vinchon, C., Sylvain, J.P., Joan, V., Tegyey, M., Clavez J.Y. and Lagny, P. (1989) Les minéralisations aurifères de l'Afrique de l'Ouest; leurs relations avec l'évolution lithostructurale au protérozoïque inférieur. *Chronique de la Recherche Minière*, **497**, 3-98.

[32] BRGM/RP-52066-FR (2003) Guide méthodologique de l'arsenic appliqué à la gestion des sites et sols pollués. 56.